

---

# Meta-LoRA: Meta-Learning LoRA Components for Domain-Aware ID Personalization

---

**Barış Batuhan Topal**

Pixery Labs

İstanbul, Türkiye

barisbatuhantopal@gmail.com

**Umut Özyurt**

METU Dept. of Computer Engineering

Ankara, Türkiye

umut.ozyurt@metu.edu.tr

**Zafer Doğan Budak**

METU Dept. of Electrical and Elec. Engineering

Ankara, Türkiye

zafer.budak@metu.edu.tr

**Ramazan Gokberk Cinbis**

METU Dept. of Computer Engineering

Ankara, Türkiye

gcinbis@metu.edu.tr

## Abstract

Recent advancements in text-to-image generative models, particularly latent diffusion models (LDMs), have demonstrated remarkable capabilities in synthesizing high-quality images from textual prompts. However, achieving identity personalization—ensuring that a model consistently generates subject-specific outputs from limited reference images—remains a fundamental challenge. To address this, we introduce Meta-Low-Rank Adaptation (Meta-LoRA), a novel framework that leverages meta-learning to encode domain-specific priors into LoRA-based identity personalization. Our method introduces a structured three-layer LoRA architecture that separates identity-agnostic knowledge from identity-specific adaptation. In the first stage, the LoRA Meta-Down layers are meta-trained across multiple subjects, learning a shared manifold that captures general identity-related features. In the second stage, only the LoRA-Mid and LoRA-Up layers are optimized to specialize on a given subject, significantly reducing adaptation time while improving identity fidelity. To evaluate our approach, we introduce Meta-PHD, a new benchmark dataset for identity personalization, and compare Meta-LoRA against state-of-the-art methods. Our results demonstrate that Meta-LoRA achieves superior identity retention, computational efficiency, and adaptability across diverse identity conditions. Our code, model weights, and dataset are released on [barisbatuhan.github.io/Meta-LoRA](https://barisbatuhan.github.io/Meta-LoRA).

## 1 Introduction

Text-to-image generative models have seen significant advancements in recent years, demonstrating a remarkable ability to generate high-quality images from textual prompt encodings [22]. Among them, latent diffusion models (LDMs) [23, 27, 15, 21] have proven to be particularly effective, utilizing deep learning to iteratively refine images within a latent space. However, achieving identity personalization—generating images that accurately capture a specific subject’s likeness while maintaining generalization—from a single or few image(s) remains a significant challenge [35].

The mainstream approaches to generative model personalization fall broadly into two extremes. On the one end, methods such as DreamBooth [24] and textual inversion [6] rely on general-purpose fine-tuning algorithms for personalization purposes. While effective in many scenarios, these methods rely purely on the priors embedded into the pre-trained generative model. Such priors, however, often provide insufficient specialization for capturing subtle domain-specific nuances, such as fine facial details. To overcome such limitations, it is commonly necessary to use a rich set of subject examples

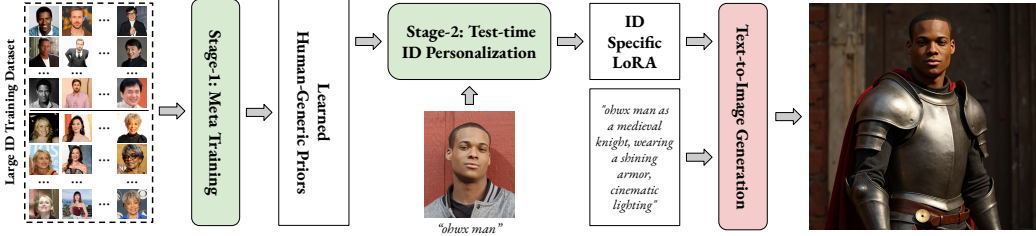


Figure 1: Our overall pipeline. In the first stage (meta-learning), we learn a subset of LoRA components capturing domain-specific priors, shared across the identities. In the second stage (personalization), only the identity-specific LoRA components are fit from a single image.

and update significant portions of model parameters in order to achieve accurate identity adaptation. Parameter-efficient fine-tuning techniques, e.g. Low-Rank Adaptation (LoRA) [10] and its variants [8, 1, 16, 34, 12], attempt to reduce adaptation complexity by constraining parameter updates through carefully designed structures; however, since these are general fine-tuning techniques, they share many of the limitations of the traditional fine-tuning techniques.

At the other extreme, feed-forward conditioning-based approaches [32, 17, 20, 9, 29, 30] train ControlNet-like [33] mechanisms to adapt generative models on-the-fly, circumventing the need for iterative fine-tuning at test time. Although appealing due to their tuning-free adaptation ability, these methods require large-scale training datasets and complex conditioning networks. In addition, their purely feed-forward structure practically limits their ability to capture fine-grained identity details.

In our work, we aim to combine the advantages of these two paradigms, blending the capability of learning domain-specific personalization priors without relying solely on computationally demanding feed-forward conditioning modules. To our knowledge, the only work that closely aligns with this direction is HyperDreamBooth [25]. HyperDreamBooth introduces a hyper-network architecture trained to predict identity-specific LoRA weights from input images, which can then be fine-tuned. However, this design necessitates a large meta-model to map input images to all per-layer LoRA components, inheriting similar drawbacks to pure feed-forward conditioning models: susceptibility to overfitting and challenging training requirements.

To overcome the limitations discussed above, we propose Meta-Low-Rank Adaptation (Meta-LoRA), a novel framework that significantly enhances LoRA-based identity personalization in text-to-image generative models, while maintaining simplicity. Specifically, we propose a structured meta-learning strategy to pre-train a subset of LoRA components in a subject-independent manner, effectively encoding domain-specific priors. This results in a compact, ready-to-adapt LoRA structure that facilitates efficient and precise adaptation to novel identities; avoiding high-complexity modules transforming images to adaptation layers used in prior work [32, 17, 20, 9, 29]. Since our meta-learning yields low-complexity LoRA components, it substantially reduces the required training dataset size compared to prior conditioning-based approaches. Furthermore, the final personalization stage involves a straightforward fine-tuning mechanism that naturally supports a variety of customizations, such as augmentations and using additional losses.

Our method introduces two key innovations compared to conventional LoRA strategies. First, Meta-LoRA employs a three-layer LoRA architecture, designed specifically to facilitate effective manifold learning of the identity domain. The *LoRA Meta-Down* layer is trained to project inputs onto a domain-specific manifold within the generative model’s feature space, capturing generic identity features shared across individuals. This learned manifold then serves as a foundation for efficiently specializing the subsequent *LoRA Mid* and *LoRA Up* layers to individual identities. Second, we adopt a structured two-stage training pipeline: initially, the Meta-Down layer is meta-trained using multiple identities to encode robust domain-specific priors, effectively establishing a generalized feature representation. Subsequently, for a given target identity, we fine-tune only the compact LoRA Mid and LoRA Up layers using only a single (or a small set of) example image(s), resulting in rapid and accurate personalization. This approach not only improves identity preservation and adaptability but also significantly reduces computational complexity and the amount of data required for personalization. An overview is given in Figure 1.

We evaluate the proposed approach with a focus on the FLUX.1-dev model [15], a state-of-the-art text-to-image diffusion system known for its high image quality and strong prompt adherence. Following prior studies, we assess personalized models trained with Meta-LoRA based on (i) the fidelity of generated faces to target identities and (ii) the prompt following abilities. However, our analysis highlights inconsistencies in recent literature regarding dataset choices and evaluation protocols, particularly the problematic reuse of the same image for both personalization and evaluation, which inflates performance estimates. To address these issues, we introduce Meta-PHD, a robust benchmark featuring diverse identities across multiple sources, with varied poses, lighting, and backgrounds, ensuring a rigorous evaluation of identity personalization methods. Our qualitative analysis further complements the quantitative results, capturing subtle yet significant details that conventional metrics may overlook. Together, our results demonstrate that the proposed approach not only preserves identity across diverse scenarios but also maintains strong generalization and prompt adherence, highlighting the potential of meta-learning for enhancing LoRA-based identity personalization.

In summary, our contributions are: (1) a novel Meta-LoRA architecture that separates generic and identity-specific components, (2) a meta-learning strategy, and an effective optimization algorithm, which enables one-shot personalization and reduces the adaptation time, (3) a new benchmark dataset (Meta-PHD) for rigorous evaluation, and (4) the proposed R-FaceSim metric to measure identity retention in a reliable manner.

## 2 Related Works

Identity personalization methods can be grouped into two: fine-tuning and feed-forward conditioning based approaches. In a pioneering work, [24] introduces DreamBooth, a fine-tuning approach that balances training with a class-specific prior-preservation loss to maintain model generalization. Custom Diffusion [13] fine-tunes select cross-attention parameters for integrating novel concepts. LoRA [10] offers a parameter-efficient alternative to fine-tuning parameters directly, enabling controlled adaptation by introducing low-rank updates to the model weights. Given its widespread adoption, we focus on the original LoRA formulation, though Meta-LoRA can naturally extend to other LoRA variants, e.g. [1, 8, 16, 34, 12].

In the second group of methods, several feed-forward conditioning methods have recently been proposed (see [35] for a recent survey). For example, PortraitBooth [20], PhotoMaker [17], InstantBooth [26], PhotoVerse [3], FastComposer [31], InstantID [29], and PuLID [9] all incorporate an IP-Adapter-like design, leveraging identity-related embeddings extracted from input ID images to manipulate text-conditioned generation with various enhancements: PortraitBooth and PhotoMaker fine-tune the diffusion model, with PortraitBooth further introducing an identity loss and locational cross-attention control. InstantBooth integrates an adapter layer positioned after the cross-attention mechanism to inject conditional features into U-Net layers. InstantID employs a ControlNet module that incorporates facial landmarks and identity embeddings. FastComposer incorporates subject embeddings extracted from an image encoder in order to augment the generic text conditioning in diffusion models. In PhotoVerse, a dual-branch conditioning mechanism operates across both text and image domains, while the training is further reinforced by a facial identity loss. PuLID enhances identity preservation through ID loss and improves text-image alignment via an alignment loss. In contrast to these works, Meta-LoRA does not require training a complex conditioning model. In addition, we simply use only diffusion loss; although the incorporation of additional losses is an orthogonal direction, and can easily be incorporated into the Meta-LoRA training, if desired.

As a work mixing elements from both groups of personalization approaches, HyperDreamBooth [25] adopts a two-stage pipeline: first, a meta-module is trained to generate LoRA-like weights based on an identity image; second, these generated weights undergo fine-tuning for the specific identity. While this method aligns with our work to some extent, it introduces several limitations that hinder its scalability and applicability; as it requires training of a complex image-to-LoRAs mapping network, expressed by a recurrent transformer architecture. In contrast, we propose to simply meta-learn a subset of LoRA components to embed domain-specific priors.

Finally, we should note that our work has been inspired by the prior work on meta-learning for classification and reinforcement learning tasks. We similarly embrace the meta-learning for fast-adaptation idea pioneered by MAML [5]. The formulation and technical details of Meta-LoRA, however, are vastly different virtually in all major ways.

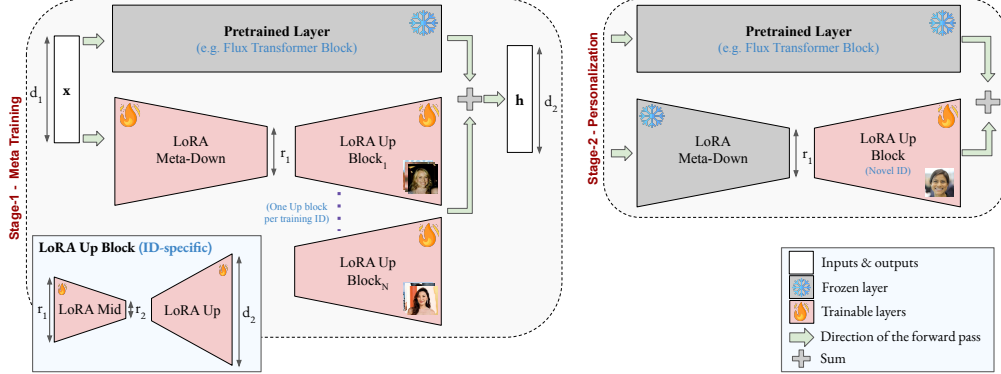


Figure 2: Proposed Meta-LoRA architecture. LoRA Meta-Down components correspond to the identity-independent LoRA components providing the domain priors into the LoRA structure. LoRA Up Blocks are defined in an identity-specific manner. During meta-training (Stage 1), the LoRA Meta-Down components are trained, along with the temporary LoRA Up Blocks corresponding to the training IDs. During testing, for a novel ID, a new set of LoRA Up Blocks are initialized and trained, while LoRA Meta-Down layers are kept frozen.

### 3 Methodology

In this section, we provide a detailed explanation of Meta-LoRA, including the model structure and an efficient training algorithm.

**Preliminaries.** In diffusion-based text-to-image (T2I) models, Low-Rank Adaptation (LoRA) [10] is primarily integrated into the attention mechanisms of the U-Net backbone, particularly within the cross-attention layers that facilitate interactions between latent image representations and text embeddings. By incorporating low-rank decomposition matrices into the weight update process, LoRA enables efficient fine-tuning while minimizing modifications to the original model parameters. In more advanced architectures, such as Stable Diffusion XL [21] and FLUX.1 [15], LoRA may also be applied to transformer-based components, enhancing latent feature extraction and improving T2I coherence. By limiting adaptation to these critical layers, LoRA optimizes parameter efficiency while maintaining the integrity of the underlying diffusion model.

We integrate our Meta-LoRA architecture into FLUX.1-dev, a state-of-the-art T2I generation model. However, the Meta-LoRA design follows a generic approach, making it adaptable to other models with similar architectures.

**Meta-LoRA Architecture.** We propose a three-layer adaptation framework by re-defining the original LoRA Down-block as an identity-shared adaptation component, which we call LoRA Meta-Down (LoMD), and decomposing the conventional LoRA Up-block into two sub-components, which we call LoRA Mid (LoM) and LoRA Up (LoU). Specifically, given some pre-trained linear layer  $W_0 : \mathcal{R}^{d_1} \rightarrow \mathcal{R}^{d_2}$  and its input  $x$ , Meta-LoRA applies the following residual update:

$$h = W_0 x + \Delta W x = W_0 x + L_{\text{up}}^i L_{\text{mid}}^i L_{\text{meta-down}} x \quad (1)$$

where  $L_{\text{meta-down}}$ ,  $L_{\text{mid}}^i$ , and  $L_{\text{up}}^i$  correspond to LoMD, LoM and LoU, respectively. The index  $i \in \{1, \dots, N\}$  indicates the identity among  $N$  training identities.

Each LoMD component serves as an identity-independent module shared across all identities to model the personalization manifold for the targeted domain (Figure 2, left). Once trained, LoMD remains frozen during test-time personalization, acting as a learned prior that facilitates rapid adaptation (Figure 2, right). The second and third components, LoM and LoU, are identity-specific, and therefore, parameterized separately for each identity. LoM reduces the output dimension of LoMD from  $r_1$  to a lower-rank representation  $r_2$ , improving efficiency while retaining relevant features, whereas LoU transforms this reduced representation back to the same dimensionality ( $d_2$ ) as the output of the pre-trained layer  $W_0$ , ensuring compatibility with the base model.

**Training overview.** Our training pipeline comprises two main stages: meta-training and test-time ID personalization. During meta-training, we learn a shared LoRA Meta-Down (LoMD) module for general features while employing distinct LoRA Mid (LoM) and LoRA Up (LoU) layers for character-specific details. In the test-time personalization stage, we fine-tune the LoM and LoU layers based on the given identity image. The following subsections provide a detailed explanation of each stage.

**Stage-1: Meta-Training.** The key challenge in the meta-training stage is learning a robust meta-representation in LoMD, while preventing under- or overfitting in the identity-specific LoM and LoU layers. A simple training approach could be optimizing all LoRA components simultaneously, for all characters. However, it is not possible to construct batches large enough to cover all identities. Trying to naively remedy this problem by applying stochastic gradient descent to the LoM and LoU components of only the identities available in each batch (and the shared LoMD parameters) also yields poor training efficiency, since the identity-specific parameters are updated much less frequently than the shared ones, resulting in poor gradients for LoMD updates.

To achieve efficient training with small batch sizes, we divide the dataset into buckets, each containing a subset of training identities. To minimize the I/O overhead, we make model updates for  $q_{\text{bucket}}$ -many iterations using each bucket data. We note that buckets can contain data larger than the maximum batch size that the VRAM allows.

Importantly, at the beginning of a new bucket, we first apply an adaptive *warm-up procedure*: in the first  $q_{\text{warm-up}}$  iterations of a new bucket, only the LoM and LoU layers corresponding to the bucket contents are updated, syncing them with the current status of the LoMD components.

In practice, we set  $q_{\text{bucket}}$  such that each example in a bucket is utilized for 10 iterations. We set  $q_{\text{warm-up}} = 0.4 \cdot q_{\text{bucket}}$  empirically to ensure that LoMD is updated only after the character-specific layers have sufficiently adapted. In the remaining iterations, LoMD is refined using more informative gradients, ensuring that the learned meta-representation continues to improve without being biased by individual identities. For all model updates, we simply use the latent-space diffusion loss  $\mathcal{L}_{\text{diff}}$ .

This structured approach prevents poor generalization due to under-trained identity-specific layers, while also mitigating the risk of overfitting. Throughout the meta-training stage, LoMD modules accumulate the common domain knowledge from which all individual-specific personalized models are expressed. At the end of this phase, all trained LoM and LoU components are discarded, and only LoMD components are retained.

**Stage-2: Test-time ID Personalization.** In the second stage, we train only the LoM and LoU layers using a novel target identity image, while keeping the LoMD weights frozen. The  $r_1$  dimension (i.e., the LoMD output dimension) remains unchanged, whereas  $r_2$  (i.e., the LoM output dimension) is set to empirically determined small values to mitigate overfitting due to the single-image input. To further prevent overfitting on a single image, we apply data augmentations. First, we detect the face in the image and determine the longer side length of the facial bounding box ( $f_{\text{long}}$ ). Then, we create multiple crops of the image using common aspect ratios: 16:9, 4:3, 1:1, 3:4, and 9:16. For each aspect ratio, we center the face and set the shorter side of the cropped image to one of the following values:  $f_{\text{long}} \cdot \{1.5, 2, 2.5, 3.5, 4.5\}$ . If the original image does not support a specific crop size, we select the closest possible size if an image with that size is not extracted. Additionally, We apply random horizontal flips to each image. In total, we generate up to 25 augmented images from a single input.

Although our focus is one-shot personalization, Meta-LoRA naturally extends to settings with multiple reference images. In such cases, the  $r_2$  dimension can be increased to enhance model capacity, potentially improving identity fidelity - a promising direction for future exploration. Finally, for simplicity, the final model can be converted back into the default LoRA structure by multiplying the LoMD and LoM matrices, producing a rank- $r_2$  (rank-1 in our experiments) LoRA model. All results presented in this paper are obtained using this conversion.

## 4 Experiments

In this section, we evaluate our approach through both quantitative and qualitative analyses, comparing it against state-of-the-art text-to-image personalization methods. We begin by describing the evaluation dataset, experimental setup, and metrics, followed by a presentation of comparative results

and corresponding discussions. The main paper focuses on the '*female*' class, as it provides more instances for stage-1 training. Evaluations on '*male*' are included in the Supplementary Material.

#### 4.1 Benchmark data set

To rigorously assess personalization performance, we curated a new test dataset, termed the **Meta-LoRA Personalization of Humans Dataset (Meta-PHD)**. This dataset comprises two complementary parts—drawn from FFHQ [11] and <https://unsplash.com/> and includes both image and prompt collections designed to challenge the model’s ability to preserve identity and adhere to diverse textual prompts. We will make the Meta-PHD dataset publicly available to facilitate fair comparisons.

**Meta-PHD-FFHQ images.** The Meta-PHD-FFHQ component contains 60 high-quality face images (30 male and 30 female) selected from the FFHQ test set [11]. Instead of utilizing the publicly available Unsplash-50 dataset as in the previous studies [7, 9], we aim to create a more diverse set that covers different range of ages and skin tones to ensure broad applicability. We applied strict selection criteria to each image: only one individual is present, the face is unobstructed (i.e., no sunglasses, hats, or hands), the eyes are open, and the head is oriented within 30 degrees of frontal.

**Meta-PHD-Unsplash images.** This component is inspired by the Unsplash-50 dataset [7] and is sourced from <https://unsplash.com/> under permissive licenses. It comprises 98 images collected from 16 identities (with 4–10 images per identity). Its main novelty is that within each identity, subjects appear in consistent attire and backgrounds but exhibit varied poses. This design ensures the dataset captures a range of views, thus preventing models from succeeding by merely replicating a single reference pose, which is foundational for the proposed R-FaceSim metric.

**Prompts.** For the FFHQ component, we prepared 20 prompts per gender (with some overlap) to test the model’s ability to generate both stylistic transformations and recontextualizations. These prompts, inspired by prior work [25, 29, 32, 9, 26], evaluate both prompt adherence and identity preservation. For the Unsplash component, we designed 10 prompts per identity focusing on pose and background variations while enforcing a frontal, unobstructed view of the subject. An example prompt is: *"A man/woman standing in a sunlit urban plaza, facing directly toward the camera with a fully detailed face and direct eye contact"*. The complete prompt list is shared in the Supplementary Material.

#### 4.2 Experimental setup

**Training dataset.** We utilize a proprietary data set of male and female images with distinct identities from those in the test benchmark and train two separate models. Each individual is represented by 20 high-resolution images ( $> 720p$ ). The dataset includes 1,050 female and 400 male subjects. The dataset is diverse in terms of age, skin tone, image environments, and accessories.

**Baseline models.** We compare our method against three state-of-the-art subject-driven image generation models: InstantID [29], PhotoMaker [17], and PuLID [9]. To ensure a fair comparison, we align evaluation conditions wherever applicable. We also benchmark against a standard LoRA baseline, both with and without augmented training data. Additional details on the baselines, including diffusion backbones and other implementation specifics, are provided in the Supplementary Material.

**Implementation details.** We trained the Stage-1 Meta-LoRA model for 50,000 iterations, on a single A6000 GPU. For the Stage-2 training, we present our results on several iterations between 250 and 750, and on ranks  $\in \{1, 2, 4, 8, 16\}$ . For the visual results, we fix the rank as 1 to maintain minimal model complexity and set the iteration count to 375 for Meta-LoRA and 625 for the default LoRA. These iterations are decided empirically to balance facial similarity and prompt following ability. Additional implementation details can be found in the Supplementary Material.

#### 4.3 Evaluation metrics and R-FaceSim

Following recent studies [25, 29, 9, 26, 24], we use two key metrics to evaluate performance: *CLIP-T* to measure the prompt following ability and the newly proposed *Robust Face Similarity (R-FaceSim)* to analyze the face similarity. The details of CLIP-T is given in the Supplementary Material.

The commonly used FaceSim metric aims to evaluate how well the generated images maintain the subject’s identity based on the cosine similarity between the reference and generated images. The facial embeddings are obtained using the backbone of a face recognition model. However, we observe two major limitations with it. First, facial recognition methods primarily learn to distinguish individuals, therefore, their embeddings rather tend to lack some of the fine-grained identity details, also observed by [4, 25, 14] in various contexts. Second, commonly the same reference images are used for both personalization and face similarity evaluation. However, in feed-forward personalization models, e.g. InstantID [29] and PuLID [9], we observe a bias towards generating images with the same pose and/or gaze as the reference images. This phenomenon indicates an undesirable limitation of those models. It also tends to artificially inflate the face-similarity scores, because the face recognition embeddings are sensitive to having the same pose or gaze.

To address the former issue, we provide a detailed discussion of the qualitative results. To address the latter one, we propose a novel face-similarity metric that we call *Robust Face Similarity (R-FaceSim)*. R-FaceSim is computed by excluding the reference image (used for fine-tuning or output-conditioning); we instead compare each generated image to other real images of the same person (with different poses) and average the cosine similarity. This yields a face-similarity score not inflated by the exact reference image. We encourage future research to adopt this approach to improve the inflated scores from pose copying as acknowledged in [7].

#### 4.4 Quantitative Results

Figure 3 provides a quantitative comparison of Meta-LoRA against the previously mentioned baselines on the ‘female’ partition of Meta-PHD test set. Our evaluation focuses on two key aspects: CLIP-T, which assess prompt adherence; and R-FaceSim, which measures identity preservation.

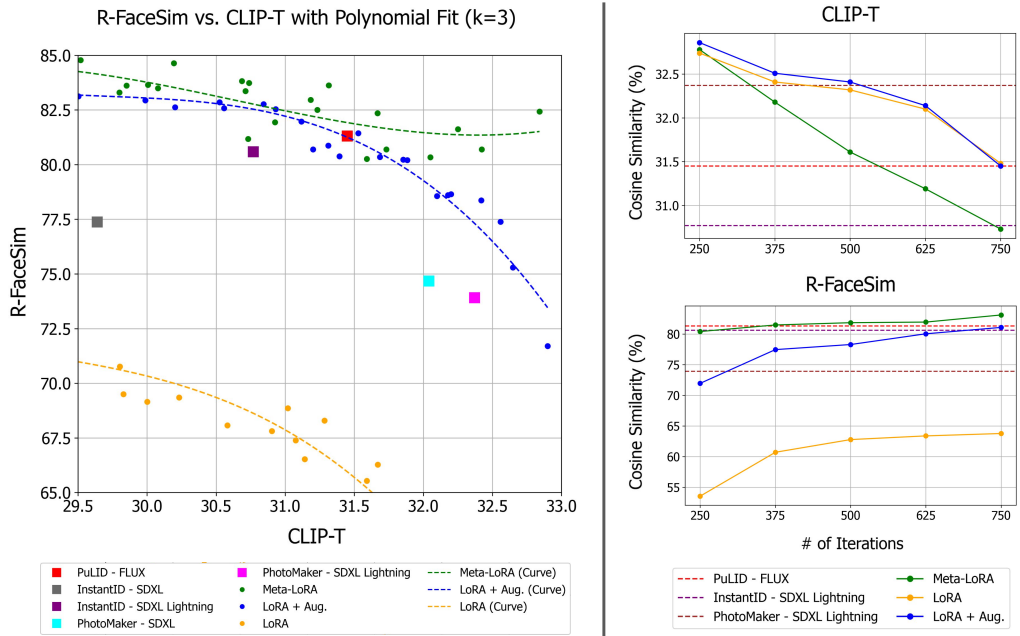


Figure 3: Illustration of the metric score trends for Meta-LoRA and the standard LoRA [10] models on the Meta-PHD dataset, focusing on the ‘female’ class. **Left:** A plot of R-FaceSim versus CLIP-T scores for all LoRA and Meta-LoRA models trained with ranks  $\in \{1, 2, 4, 8, 16\}$  and across 250, 375, 500, 625, and 750 training iterations. The polynomial fit curves per each model are also shared for better comparison. **Right:** R-FaceSim and CLIP-T scores plotted against iteration count for rank-1 LoRA and Meta-LoRA models. These results are compared with state-of-the-art models from the literature, including PuLID [9], InstantID [29], and PhotoMaker [17]. To ensure a fair comparison, we use the FLUX.1-dev version of PuLID [15], which is consistent with the Meta-LoRA training setup. InstantID and PhotoMaker are based on SD-XL [21] and SD-XL Lightning [18], as public implementations of these models are not currently available for FLUX.1-dev.

Base models are typically trained for broad, general-purpose tasks, so fine-tuning them for identity personalization can compromise their prompt following ability—often leading to lower CLIP-T scores. Conversely, overfitting to a reference identity can improve R-FaceSim but at the expense of generalization. Striking a balance between these two objectives remains a challenge for existing identity personalization methods. For example, InstantID [29] and PhotoMaker [17] tend to favor one over the other: PhotoMaker achieves higher CLIP-T scores but compromises identity preservation, while InstantID emphasizes facial similarity at the cost of broader alignment. In contrast, PuLID [9] and our proposed Meta-LoRA demonstrate a more effective balance between identity fidelity and generalization.

On Figure 3 (Left), the training results of *Meta-LoRA* occupy a higher position on the R-FaceSim vs. CLIP-T plot compared to all other models. Its polynomial trendline outperforms the rest, with LoRA+Augmentation (Aug) and PuLID being the closest in performance. While *LoRA+Aug* achieves results comparable to PuLID, the default *LoRA* lags behind all competitors, underscoring the value of data augmentation. Moreover, *Meta-LoRA* exhibits more stable R-FaceSim values across varying CLIP-T scores, unlike *LoRA+Aug*. This suggests that *Meta-LoRA* trains more consistently and learns facial features faster, as evidenced by higher CLIP-T scores in earlier training stages.

On Figure 3 (Right), the effect of iteration count on CLIP-T and R-FaceSim is shown. The plots reveal an inverse relationship between the two metrics. *Meta-LoRA* captures facial features more quickly than other LoRA variants, highlighting the efficiency of its meta-learned components in reducing adaptation time. However, this comes at the cost of slightly lower text-image alignment performance when compared at the same iteration. Still, between iterations 375 and 500, *Meta-LoRA* outperforms PuLID on both metrics, suggesting that this range offers a more optimal balance between identity preservation and text alignment. Additional comparisons are given in the Supplementary Material.

Another key difference lies in the scale of pretraining data and the use of additional training losses. Existing models are trained on substantially larger datasets—our dataset constitutes only 0.035% of InstantID’s, 1.4% of PuLID’s, and 18.75% of PhotoMaker’s—and none of these studies share their training data publicly. Furthermore, PuLID incorporates a face-centric identity loss, while InstantID embeds facial features directly into its network. In contrast, *Meta-LoRA* achieves comparable or superior performance without relying on such explicit facial losses or features, instead employing a simpler and more efficient training strategy.

## 4.5 Qualitative Results

To evaluate visual fidelity and prompt adherence, we qualitatively compare *Meta-LoRA* against baselines [9, 17, 10, 29], focusing on female samples due to the larger Stage-1 training dataset (male subject analysis is in Supplementary Material).

Figure 4 (left) underscores *Meta-LoRA*’s superior ability to preserve nuanced facial characteristics while robustly integrating prompt details. It uniquely achieves a compelling balance between identity retention and scene coherence, producing visually faithful and textually aligned results. In contrast, standard **LoRA** struggles with consistent identity preservation despite following prompts. **InstantID** often replicates the reference image’s pose, which, while beneficial for some prompts, significantly curtails its adaptability to diverse viewpoints or styles and can artificially inflate naive similarity metrics. **PhotoMaker** captures general likeness but often fails to render fine-grained facial details, especially when prompts demand significant contextual or stylistic shifts.

Figure 4 (right) examines robustness to seed variation. *Meta-LoRA* achieves a desirable equilibrium between seed-dependent output diversity and consistent identity fidelity. Unlike standard **LoRA**, which can overfit to incidental background features from the reference image, or **PuLID**, which shows limited variation across seeds and sometimes falters in prompt-driven facial modifications, *Meta-LoRA* generates diverse yet accurate outputs. This demonstrates its strong capability to explore varied creative outputs while maintaining high fidelity to both the subject’s identity and the textual prompt.

In essence, qualitative assessments strongly corroborate *Meta-LoRA*’s quantitative advantages. It consistently produces images that are accurate to the subject’s identity and the given prompt, preserving distinctive facial features while offering meaningful creative variation. This positions *Meta-LoRA* as

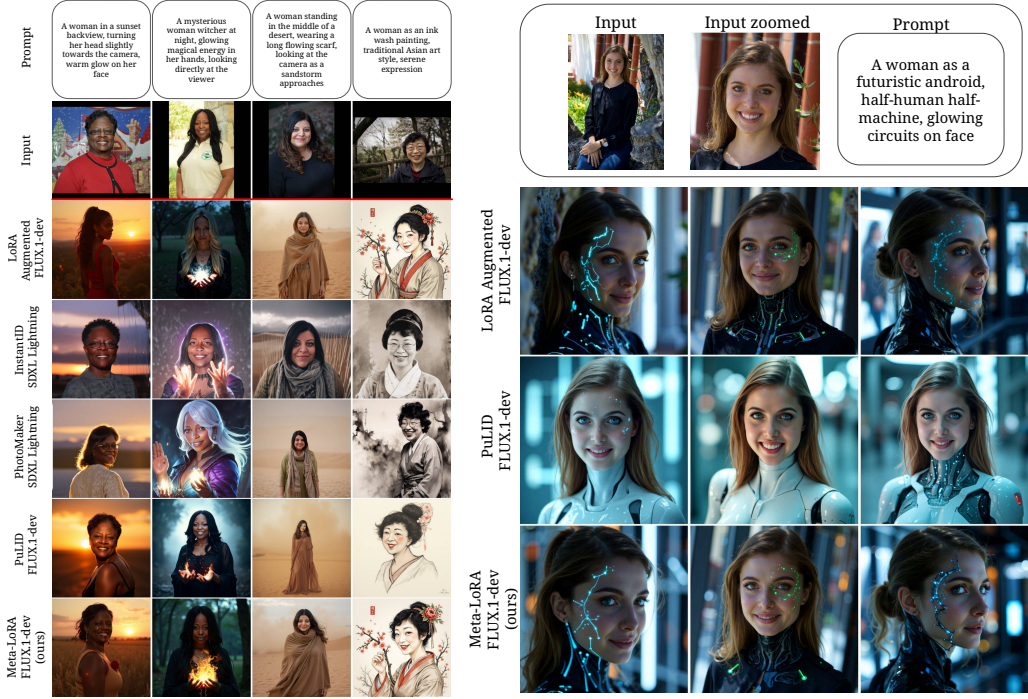


Figure 4: Qualitative comparisons. **Left:** Meta-LoRA shows better ID preservation while keeping prompt alignment. Meta-LoRA keeps the pose natural (1st column), promotes identities effectively (2nd and 3rd columns), and follows the given style (4th column). **Right:** Comparisons across different seeds. For each different seed, Meta-LoRA successfully generates distinct variations, while also preserving the prompt alignment. Details are best viewed on screen, zoomed-in.

a highly effective solution for applications demanding both strong identity preservation and versatile prompt adherence.

## 5 Conclusion

In this paper, we present Meta-Low-Rank Adaptation (Meta-LoRA), a versatile three-layer LoRA architecture designed to enhance identity personalization in text-to-image generative models. Meta-LoRA employs a two-stage training strategy: the first stage learns generic LoRA Meta-Down layers applicable across multiple identities, while the second stage fine-tunes the LoRA Mid and LoRA Up layers for a specific identity using only a single reference image. By integrating domain-specific priors and optimizing feature learning across diverse identities, Meta-LoRA significantly improves identity preservation, robustness, computational efficiency, and adaptability.

To evaluate our approach, we introduce Meta-PHD, a novel identity personalization dataset used exclusively for testing, and assess Meta-LoRA’s performance using this dataset. Our results demonstrate that Meta-LoRA achieves state-of-the-art (SOTA) performance or performs comparably to existing SOTA methods. Moreover, qualitative evaluations highlight Meta-LoRA’s ability to generate identity-personalized images while effectively maintaining prompt adherence. Future research directions include the incorporation of recent LoRA variants [8, 1, 16, 34, 12] into the Meta-LoRA framework and the exploration of the proposed method’s applicability to other model customization tasks.

## Acknowledgments

This work was supported in part by the METU Research Fund Project ADEP-312-2024-11525 and BAGEP Award of the Science Academy. The numerical calculations reported in this paper were partially performed using the MareNostrum 5 pre-exascale supercomputing system. We gratefully

acknowledge the Barcelona Supercomputing Center (BSC) and the Scientific and Technological Research Council of Turkey (TÜBİTAK) for providing access to these resources and supporting this research. We also gratefully acknowledge the computational resources kindly provided by METU ImageLab and METU ROMER.

## References

- [1] S. Borse, S. Kadambi, N. Pandey, K. Bhardwaj, V. Ganapathy, S. Priyadarshi, R. Garrepalli, R. Esteves, M. Hayat, and F. Porikli. Foura: Fourier low-rank adaptation. In *NeurIPS*, 2024.
- [2] Q. Cao, L. Shen, W. Xie, O. M. Parkhi, and A. Zisserman. Vggface2: A dataset for recognising faces across pose and age. In *IEEE Int. Conf. on Automatic Face & Gesture Recognition*, pages 67–74. IEEE, 2018.
- [3] L. Chen, M. Zhao, Y. Liu, M. Ding, Y. Song, S. Wang, X. Wang, H. Yang, J. Liu, K. Du, et al. Photoverse: Tuning-free image customization with text-to-image diffusion models. *arXiv preprint arXiv:2309.05793*, 2023.
- [4] X. Chen, K. He, J. Zhu, Y. Ge, W. Li, and C. Wang. Hifivfs: High fidelity video face swapping. *arXiv preprint arXiv:2411.18293*, 2024.
- [5] C. Finn, P. Abbeel, and S. Levine. Model-agnostic meta-learning for fast adaptation of deep networks. In *ICML*, 2017.
- [6] R. Gal, Y. Alaluf, Y. Atzmon, O. Patashnik, A. H. Bermano, G. Chechik, and D. Cohen-or. An image is worth one word: Personalizing text-to-image generation using textual inversion. In *The Eleventh International Conference on Learning Representations*, 2023.
- [7] R. Gal, O. Lichter, E. Richardson, O. Patashnik, A. H. Bermano, G. Chechik, and D. Cohen-Or. Lcm-lookahead for encoder-based text-to-image personalization. In *ECCV*, pages 322–340. Springer, 2024.
- [8] Z. Gao, Q. Wang, A. Chen, Z. Liu, B. Wu, L. Chen, and J. Li. Parameter-efficient fine-tuning with discrete fourier transform. In *ICML*, 2024.
- [9] Z. Guo, Y. Wu, Z. Chen, L. chen, P. Zhang, and Q. HE. PuLID: Pure and lightning ID customization via contrastive alignment. In *The Thirty-eighth Annual Conference on Neural Information Processing Systems*, 2024.
- [10] E. J. Hu, Y. Shen, P. Wallis, Z. Allen-Zhu, Y. Li, S. Wang, L. Wang, W. Chen, et al. Lora: Low-rank adaptation of large language models. In *ICLR*, 2022.
- [11] T. Karras, S. Laine, and T. Aila. A style-based generator architecture for generative adversarial networks. In *Proceedings of the IEEE/CVF conference on computer vision and pattern recognition*, pages 4401–4410, 2019.
- [12] D. J. Kopiczko, T. Blankevoort, and Y. M. Asano. Vera: Vector-based random matrix adaptation. In *ICLR*, 2024.
- [13] N. Kumari, B. Zhang, R. Zhang, E. Shechtman, and J.-Y. Zhu. Multi-concept customization of text-to-image diffusion. In *CVPR*, pages 1931–1941, 2023.
- [14] H.-W. Kung, T. Varanka, S. Saha, T. Sim, and N. Sebe. Face anonymization made simple. *arXiv preprint arXiv:2411.00762*, 2024.
- [15] B. F. Labs. Flux. <https://github.com/black-forest-labs/flux>, 2024.
- [16] Y. Li, S. Han, and S. Ji. Vb-lora: Extreme parameter efficient fine-tuning with vector banks. In *NEURIPS*, 2024.
- [17] Z. Li, M. Cao, X. Wang, Z. Qi, M.-M. Cheng, and Y. Shan. Photomaker: Customizing realistic human photos via stacked id embedding. In *CVPR*, pages 8640–8650, 2024.

- [18] S. Lin, A. Wang, and X. Yang. Sdxl-lightning: Progressive adversarial diffusion distillation. *arXiv preprint arXiv:2402.13929*, 2024.
- [19] I. Loshchilov. Decoupled weight decay regularization. *arXiv preprint arXiv:1711.05101*, 2017.
- [20] X. Peng, J. Zhu, B. Jiang, Y. Tai, D. Luo, J. Zhang, W. Lin, T. Jin, C. Wang, and R. Ji. Portraitbooth: A versatile portrait model for fast identity-preserved personalization. In *CVPR*, pages 27080–27090, 2024.
- [21] D. Podell, Z. English, K. Lacey, A. Blattmann, T. Dockhorn, J. Müller, J. Penna, and R. Rombach. SDXL: Improving latent diffusion models for high-resolution image synthesis. In *The Twelfth International Conference on Learning Representations*, 2024.
- [22] A. Radford, J. W. Kim, C. Hallacy, A. Ramesh, G. Goh, S. Agarwal, G. Sastry, A. Askell, P. Mishkin, J. Clark, et al. Learning transferable visual models from natural language supervision. In *ICML*, pages 8748–8763. PMLR, 2021.
- [23] R. Rombach, A. Blattmann, D. Lorenz, P. Esser, and B. Ommer. High-resolution image synthesis with latent diffusion models. In *CVPR*, pages 10684–10695, 2022.
- [24] N. Ruiz, Y. Li, V. Jampani, Y. Pritch, M. Rubinstein, and K. Aberman. Dreambooth: Fine tuning text-to-image diffusion models for subject-driven generation. In *CVPR*, pages 22500–22510, 2023.
- [25] N. Ruiz, Y. Li, V. Jampani, W. Wei, T. Hou, Y. Pritch, N. Wadhwa, M. Rubinstein, and K. Aberman. Hyperdreambooth: Hypernetworks for fast personalization of text-to-image models. In *CVPR*, 2024.
- [26] J. Shi, W. Xiong, Z. Lin, and H. J. Jung. Instantbooth: Personalized text-to-image generation without test-time finetuning. In *CVPR*, 2024.
- [27] Stability AI. Introducing stable diffusion 3.5, 2024.
- [28] C. Szegedy, S. Ioffe, V. Vanhoucke, and A. Alemi. Inception-v4, inception-resnet and the impact of residual connections on learning. In *AAAI*, volume 31, 2017.
- [29] Q. Wang, X. Bai, H. Wang, Z. Qin, A. Chen, H. Li, X. Tang, and Y. Hu. Instantid: Zero-shot identity-preserving generation in seconds. *arXiv preprint arXiv:2401.07519*, 2024.
- [30] Y. Wei, Y. Zhang, Z. Ji, J. Bai, L. Zhang, and W. Zuo. Elite: Encoding visual concepts into textual embeddings for customized text-to-image generation. In *CVPR*, pages 15943–15953, 2023.
- [31] G. Xiao, T. Yin, W. T. Freeman, F. Durand, and S. Han. Fastcomposer: Tuning-free multi-subject image generation with localized attention. *IJCV*, pages 1–20, 2024.
- [32] H. Ye, J. Zhang, S. Liu, X. Han, and W. Yang. Ip-adapter: Text compatible image prompt adapter for text-to-image diffusion models, 2023.
- [33] L. Zhang, A. Rao, and M. Agrawala. Adding conditional control to text-to-image diffusion models. In *CVPR*, pages 3836–3847, 2023.
- [34] Q. Zhang, M. Chen, A. Bukharin, P. He, Y. Cheng, W. Chen, and T. Zhao. Adaptive budget allocation for parameter-efficient fine-tuning. In *ICLR*, 2023.
- [35] X. Zhang, X.-Y. Wei, W. Zhang, J. Wu, Z. Zhang, Z. Lei, and Q. Li. A survey on personalized content synthesis with diffusion models. *arXiv preprint arXiv:2405.05538*, 2024.

# Meta-LoRA: Meta-Learning LoRA Components for Domain-Aware ID Personalization

## Appendix

This document presents supplementary discussions and additional details that extend the main paper.

### A Implementation Details

Meta-LoRA is implemented using the ai-toolkit<sup>1</sup> framework. Training and evaluation are performed on a single NVIDIA RTX A6000 GPU with 48GB of VRAM (see Section C for details). Under this setup, Stage-1 training takes approximately 7 days (13 seconds per iteration for a total of 50,000 iterations), while Stage-2 training takes around 18 minutes (2.8 seconds per iteration for 375 iterations).

For all training runs, we use a learning rate of 0.0004, set the total number of Stage-1 iterations ( $q_{total}$ ) to 50,000, bucket size ( $q_{bucket}$ ) to 2,500, warm-up iterations ( $q_{warm-up}$ ) to 1,000, and Stage-2 iterations ( $q_{st2}$ ) to 375. To analyze performance across configurations, we evaluate both Meta-LoRA and the default LoRA at different ranks  $\in \{1, 2, 4, 8, 16\}$  and checkpoints  $\in \{250, 375, 500, 625, 750\}$ . Batch sizes are set to 4 for Stage-1 and 1 for Stage-2. Training is performed using the standard L2 loss, and we use the AdamW optimizer [19].

### B Meta-Training and Personalization Algorithms

In this subsection, we give the algorithms for the proposed meta-training and test-time ID personalization stages. The algorithm for the first stage is shared in Algorithm 1, and for the second stage in Algorithm 2. A detailed explanation of these stages can be found in Section 3 of the actual paper.

---

**Algorithm 1:** Stage-1 - Meta Training

---

**Input:**

- $buckets$ : the training dataset with the characters are grouped in buckets
- $r_1, r_2$ : Lora Down and Lora Mid output dimensions -  $N$ : number of characters per bucket
- $q_{bucket}$ : number of iterations with each bucket
- $q_{total}$ : number of total iterations
- $q_{warm-up}$ : iterations to only update LoM and LoU
- $bs$ : batch size

**Output:** Stage-1 weights of Meta-LoRA

```
model  $\leftarrow$  Meta-LoRA.initialize( $r_1, r_2, N$ ) ;  
 $i_{curr} \leftarrow 0$ ;
```

```
while  $i_{curr} < q_{total}$  do  
    for  $bucket$  in  $buckets$  do  
        data  $\leftarrow$  Dataloader( $bucket, bs$ ) ;  
         $i_{cb} \leftarrow 0$ ;  
        for  $batch$  in  $data$  and  $i_{cb} < q_{bucket}$  do  
            loss  $\leftarrow$  model( $batch$ );  
            if  $i_{cb} < q_{warm-up}$  then  
                update-mid-and-up-layers( $loss$ );  
            else  
                update-model( $loss$ );  
             $i_{cb} \leftarrow i_{cb} + 1$ ;  
         $i_{curr} \leftarrow i_{curr} + i_{cb}$ ;
```

---

```
return model
```

---

<sup>1</sup><https://github.com/ostris/ai-toolkit>

---

**Algorithm 2:** Stage-2 - Test-time ID Personalization

---

**Input:**

- $image_{person}$ : the single image of the person to learn
- $r_1, r_2$ : LoRA Down and Mid output dimensions
- $q_{st2}$ : Number of iterations
- $weights_{st1}$ : Stage-1 LoRA Down weights

**Output:**  $weights_{final}$ : Final Meta-LoRA Weights

```
model ← Meta-LoRA.initialize( $r_1, r_2, N$ ) ;
load-down-weights(model,  $weights_{st1}$ );
dataset ← augment-and-create-data( $image_{person}$ );
for iter = 1 to  $q_{st2}$  do
    for item in dataset do
        loss ← model(batch);
        update-mid-and-up-layers(loss);
```

**return**  $model$ 

---

## C Baseline Model Details and Implementation Settings

**Model variants and base diffusion backbones.** We evaluate our Meta-LoRA personalization approach against several state-of-the-art subject-driven generation methods with publicly available implementations: InstantID [29], PhotoMaker [17], and PuLID [9]. As a FLUX.1-dev-based [15] implementation of PuLID is available, which is claimed to improve upon the original paper’s version (i.e., `FLUX_PuLID_v0.9.1` from its public repository<sup>2</sup>), we use this version for a direct comparison. For InstantID and PhotoMaker, although their respective GitHub demos recommend different diffusion backbones, we standardize the evaluation by running all SDXL-based methods under these two base variants to ensure fairness:

- **SDXL-Base 1.0** (`stable-diffusion-xl-base-1.0`)
- **SDXL-Lightning** (`sdxl-lightning`)

In contrast, our default LoRA and Meta-LoRA approaches are built on a FLUX.1-dev-based [15] model.

**Hardware and data types.** All experiments based on SDXL are conducted on a single NVIDIA RTX 3090 GPU with 24GB VRAM. In contrast, experiments involving FLUX.1-dev models—including PuLID, LoRA, and Meta-LoRA—are run on a single NVIDIA A6000 GPU with 48GB VRAM, utilizing CPU offloading. Additionally, LoRA training and the stage-2 training of Meta-LoRA (used solely for rank-based performance analysis) are carried out on a single NVIDIA H100 GPU with 66GB VRAM. In all cases, `bf16` is used as the inference data type.

**Model-specific inference configurations.** For Meta-LoRA and each of the studies that we provide a comparison, the following configurations are selected for inference:

- **Meta-LoRA and LoRA:** `inference_steps=30, cfg=3.5, true_cfg=1.0, lora_strength=1.0`
- **PuLID:** We follow the repository’s demo code, and set `id_weight=1.0, true_cfg=1.0, time_to_start_cfg=1, inference_steps=20, cfg=4.0, and max_sequence_length=128`.
- **PhotoMaker:** We use PhotoMakerV2, which differs from the version evaluated in the PuLID paper [9] (where its performance was reported as poor, and claimed it is not even compatible with SDXL-Lightning). In our experiments, PhotoMakerV2 yields substantially improved results—possibly owing to internal updates. To ensure compatibility with SDXL-Lightning (particularly for a 4-step inference), we set `time_spacing="trailing"` in the Euler scheduler configuration and adjust the `start_merge_step` parameter to

<sup>2</sup><https://github.com/ToTheBeginning/PuLID>

0 for SDXL-Lightning or 10 for SDXL-Base. We further prepend the keyword “img” to each prompt (e.g., “man img ...”, “woman img ...”) to satisfy PhotoMaker’s trigger-word requirement.

- **InstantID:** For InstantID, we consider two implementations: **(i)** The ComfyUI-based approach used in the PuLID paper [9], which exposes a “denoise” parameter in the `kSampler` node (with values between 0 and 1). **(ii)** The original InstantID GitHub repository’s implementation. In the ComfyUI setup, a denoise value in the range (0.8, 1.0] yields consistent sigma values ( $\{14.6146, 2.9183, 0.9324, 0.0292, 0.0000\}$  for a 4-step process) and markedly improves image quality for SDXL-Lightning. In the original repository, the time-step derivation departs from the standard SDXL pipeline, resulting in underdeveloped outputs. We therefore replace this part with the official SDXL pipeline (manually applying the aforementioned sigma values) to align the results with those from the ComfyUI version. For both implementations, we set `controlnet_conditioning_scale=0.8` and `ip_adapter_scale=0.8`. In spite of employing a robust negative prompt (see below) to counteract SDXL-FLUX artifacts, InstantID outputs tend to exhibit watermarks, a reflection of the training data characteristics. Following the InstantID GitHub recommendations, we generate images at  $1016 \times 1016$  and then resize them to  $1024 \times 1024$ , which reduces watermark occurrence.

**Common inference configurations.** Below, the configuration parameters are shared, which are common to multiple models:

- **Image size:** We set the generated image size for all experiments (except InstantID) as  $1024 \times 1024$ .
- **Negative prompts:** While FLUX.1-dev-based models do not leverage any negative prompts, the following text is used for all SDXL-based methods: *“flaws in the eyes, flaws in the face, flaws, lowres, non-HDRi, low quality, worst quality, artifacts noise, text, watermark, glitch, deformed, mutated, ugly, disfigured, hands, low resolution, partially rendered objects, deformed or partially rendered eyes, deformed, deformed eyeballs, cross-eyed, blurry”*.
- **SDXL inference details:** We employ the Euler scheduler for all SDXL inferences. For SDXL-Lightning, we adopt the 4-step `sdxl-lightning` checkpoint from ByteDance’s HuggingFace page, with `CFG-scale=1.2`, following recommendations from the PuLID paper [9]. SDXL-Base 1.0, we set `CFG-scale=5.0` and use 50 inference steps, in line with standard SDXL configurations.

## D Choices of Rank and Iteration Count on Meta-LoRA and LoRA Trainings

**On the rank selection.** Although we present results across various rank values in Figure 3 (Left) of the main paper, all of our qualitative and additional quantitative analyses are conducted using rank-1 configurations. This decision is motivated by several considerations:

- Our goal is to maintain a minimal and straightforward setup, while still demonstrating that the model can effectively learn identity representations. To align with this objective, we also restrict fine-tuning to a single identity image.
- With only one image available during fine-tuning, larger model capacities (i.e., higher ranks) increase the risk of overfitting. Rank-1 offers a good trade-off between CLIP-T and R-FaceSim performance, making it a practical and effective default choice for our study. See Section I for a more detailed analysis.

That said, our framework naturally supports scenarios involving multiple identity images during fine-tuning, which can be further explored in future work. In such cases, using higher ranks may further improve and stabilize model performance.

**On the number of iterations.** As discussed in Section A, we evaluate our models across different rank values and training iterations. For Meta-LoRA, we empirically observed that iteration 375 achieves a well-balanced trade-off between prompt adherence and identity preservation—that is, the generated images accurately reflect the target identity without exhibiting noticeable overfitting to

the input image. Thanks to its Stage-1 preconditioning on identity-related information, Meta-LoRA converges more rapidly than the default LoRA architecture. In contrast, the default LoRA model reaches a similar balance around iteration 625 (i.e., identity fidelity remains underfitted at earlier iterations). Based on these findings, we select iteration 375 for Meta-LoRA Stage-2 and iteration 625 for LoRA in our main evaluations.

Although these extended and augmented LoRAs show improved performance, our Meta-LoRA—with its meta-learned prior—converges faster and achieves higher identity fidelity in fewer steps.

Table 1: Meta-PHD-FFHQ Recontextualized Prompts

Prompt
A man in a firefighter uniform, standing in front of a firetruck, looking straight ahead.
A man in a spacesuit, floating in space with Earth in the background, face clearly visible.
A 90-year-old man with completely white hair, deep wrinkles covering his forehead, around his eyes, and mouth, looking at the viewer, well-lit portrait.
A man as a 1-year-old baby, joyful and playful, looking directly at the camera, soft lighting.
A man riding a bicycle under the Eiffel Tower, smiling at the camera.
A man playing a guitar in the forest, looking at the viewer, natural lighting.
A man working on a laptop in a modern office, facing forward with focused expression.
A man as a medieval knight, wearing a shining armor, cinematic lighting.
A man in a 1920s noir setting, wearing a fedora, moody lighting.
A man standing in the middle of a desert, wearing a long flowing scarf, looking at the camera as a sandstorm approaches.
A woman in a swimming pool, water reflecting on her face, looking straight ahead.
A woman in a sunset backview, turning her head slightly towards the camera, warm glow on her face.
A woman piloting a fighter jet, cockpit reflections visible, face clearly in focus.
A woman in New York, standing in Times Square, bright city lights illuminating her face.
A woman reading books in the library, facing forward, glasses on, scholarly expression.
A woman driving a car, cityscape in the background, focused expression, looking ahead.
A woman standing in the middle of a desert, wearing a long flowing scarf, looking at the camera as a sandstorm approaches.
A woman walking along a misty cobblestone street in an old European town, holding a vintage lantern, gazing into the distance.
A woman sitting on a rooftop at dusk, overlooking a glowing city skyline, sipping from a warm cup, smiling at the camera.
A woman in a 1920s noir setting, wearing a vintage dress, moody lighting.

## E Details on Evaluation Datasets and Prompts

The FFHQ partition of the Meta-PHD dataset, along with the prompts listed in Tables 1 and 2, is used exclusively to assess the models’ prompt-following capabilities, as measured by the CLIP-T metric. These prompts include both stylistic and recontextualization examples, enabling evaluation across multiple dimensions of prompt adherence.

In contrast, the Unsplash partition and the prompts provided in Table 3 are employed to evaluate our proposed metric, R-FaceSim. These prompts are specifically crafted to encourage the generation of images in which the subject is directly facing the camera, with no facial occlusions, ensuring optimal conditions for facial similarity assessment.

## F Details on Evaluation Metrics

**CLIP-T.** CLIP-T measures how well the generated image aligns with the textual prompt. It is computed as the cosine similarity between the CLIP embeddings of the input prompt and the generated image. We use the CLIP ViT-B/32 model [22] to obtain the embeddings. A higher CLIP-T score indicates stronger prompt adherence.

Table 2: Meta-PHD-FFHQ Stylistic Prompts Examples

Prompt
A man as a cyberpunk character, neon lights reflecting on his face, highly detailed.
A man as an ink wash painting, traditional Asian art style, serene expression.
A man as a futuristic android, half-human half-machine, glowing circuits on face.
A man in an art nouveau portrait, elegant and highly stylized.
A Pixar character of a man, expressive and exaggerated facial features.
A man sculpted out of marble, photorealistic, museum lighting.
A pop-art style portrait of a man, bright colors and bold outlines.
A Funko pop figure of a man, oversized head, cartoonish features.
A pencil drawing of a man, highly detailed, face in full view.
A painting of a man in Van Gogh style, expressive brush strokes, looking at the viewer.
A woman as a cyberpunk character, neon lights reflecting on her face, highly detailed.
A woman as an ink wash painting, traditional Asian art style, serene expression.
A woman as a futuristic android, half-human half-machine, glowing circuits on face.
A woman in an art nouveau portrait, elegant and highly stylized.
A painting of a woman in Van Gogh style, expressive brush strokes, looking at the viewer.
A Pixar character of a woman, expressive and exaggerated facial features.
A woman sculpted out of marble, photorealistic, museum lighting.
A pop-art style portrait of a woman, bright colors and bold outlines.
A Funko pop figure of a woman, oversized head, cartoonish features.
A mysterious woman witcher at night, glowing magical energy in her hands, looking directly at the viewer.

**Conventional FaceSim.** Conventional FaceSim metric is computed by extracting facial embeddings from the generated images using an Inception-ResNet [28] model pre-trained on VGGFace2 [2], followed by calculating the cosine similarity between these embeddings and those of the real subject. A discussion on the shortcomings of the conventional FaceSim metric, and the proposed improved version is given in the experiments section of the main paper.

Table 3: Meta-PHD-Unsplash Prompts - FaceSim

Prompt
A [man/woman] standing in a sunlit urban plaza, facing directly toward the camera with a fully visible, highly detailed face and direct eye contact.
A [man/woman] in a casual outfit, positioned in a blooming garden with soft natural light, [his/her] face clearly visible and [his/her] eyes meeting the camera.
A [man/woman] in a minimalist, modern outfit, set against a softly lit abstract background, with [his/her] face rendered in intricate detail and direct eye contact.
A [man/woman] in elegant attire, standing against a scenic landscape at sunrise, [his/her] face captured in sharp detail with a steady, direct gaze.
A [man/woman] in a relaxed, stylish ensemble, posed on a quiet beach at sunset, with a fully visible, richly detailed face and clear eye contact.
A [man/woman] in a fashionable outfit, placed in a vibrant urban art scene, with [his/her] face prominently visible, detailed, and looking straight at the camera.
A [man/woman] with a confident expression, standing in a serene park under bright daylight, [his/her] face rendered in high detail and engaging directly with the viewer.
A [man/woman] in a chic outfit, situated in a picturesque alleyway with soft ambient lighting, with [his/her] face clearly displayed in full detail and direct gaze.
A [man/woman] in a modern, casual look, standing in a contemporary indoor space with artistic lighting, [his/her] face fully visible and rendered with intricate detail as [he/she] looks at the camera.
A [man/woman] in a trendy outfit, positioned in a lively outdoor market where natural light highlights [his/her] features, [his/her] face completely unobstructed and detailed, with direct eye contact.

**R-FaceSim.** Algorithm 3 outlines the computation of the Robust Face Similarity Metric (R-FaceSim), which leverages multiple images per identity, carefully curated prompts, and a generative text-to-image model. For each identity, one image is designated as the reference, while the remaining images constitute the test set. The model is either conditioned or fine-tuned on the reference image. For each prompt, the model generates an output image, from which the face is cropped and its identity embedding is extracted. This embedding is then compared—using cosine similarity—to the embeddings of faces from the corresponding test images. The mean similarity for a given prompt and identity is calculated by averaging these cosine similarities. The final R-FaceSim score is obtained by averaging these values across all identities and prompts. The models employed in this process are identical to those used in the *Conventional FaceSim* evaluation.

---

**Algorithm 3:** Robust Face Similarity Metric (R-FaceSim)

---

$I$  Set of identities with multiple images  
 $P$  Set of carefully chosen prompts  
**Input:**  $M$  Generative text-to-image model  
 $C$  Face cropper  
 $E$  Identity embedding extractor  
**Output:**  $R\text{-FaceSim}$ : Robust Face Similarity Score  
**for** each  $i \in I$  **do**  
     $ref \leftarrow \text{select\_one}(i);$   
     $T \leftarrow i \setminus \{ref\};$   
     $M \leftarrow \text{fine-tune}/\text{image-prompt}(M, ref);$   
    **for** each  $p \in P$  **do**  
         $g \leftarrow M(p);$   
         $f_g \leftarrow C(g);$   
         $e_g \leftarrow E(f_g);$   
         $sumsim \leftarrow 0, count \leftarrow 0;$   
        **for** each  $t \in T$  **do**  
             $f_t \leftarrow C(t);$   
             $e_t \leftarrow E(f_t);$   
             $sim \leftarrow \text{cosine}(e_g, e_t);$   
             $sumsim \leftarrow sumsim + sim;$   
             $count \leftarrow count + 1;$   
         $S(i, p) \leftarrow \frac{sumsim}{count};$   
     $R\text{-FaceSim} \leftarrow \text{mean}\{S(i, p) : i \in I, p \in P\};$   
**return**  $R\text{-FaceSim}$

---

**Justification for R-FaceSim.** As shown in Table 4, we observe a nontrivial gap between the conventional FaceSim scores and our proposed R-FaceSim scores. In particular, personalization approaches such as InstantID [29] and PuLID [9] often replicate the poses or gazes of the reference image, thereby artificially boosting FaceSim results. Meanwhile, PhotoMaker [17] is not as heavily affected by this phenomenon, as indicated by its relatively smaller discrepancy between the two metrics. Additionally, non-augmented LoRA baselines can overfit the position of the face in the generated image, further inflating their face similarity scores. This pose-copying and overfitting phenomenon conflates true identity fidelity with pose or spatial similarity, leading to overestimated accuracy in conventional FaceSim evaluations.

By contrast, R-FaceSim explicitly excludes the original reference image during evaluation and compares each generated output against multiple images of the same identity (captured under diverse conditions). This design ensures that high similarity scores genuinely reflect robust identity preservation rather than a mere replication of pose or gaze. Consequently, the observed differences in Table 4 (ranging up to 10% drop in some cases) highlight how pose-copying and overfitting can lead to inflated identity fidelity under conventional FaceSim. Our R-FaceSim metric thus offers a more stringent and realistic assessment of personalization performance, as it mitigates the bias introduced by reference-image reuse and captures fine-grained identity traits across varied visual contexts. We encourage future work to adopt this approach, especially when evaluating feed-forward or near-instant personalization methods that rely heavily on a single reference image.

Table 4: Comparison between the Robust FaceSim and FaceSim metrics, with percentage differences highlighted in cases of significant performance drops. All scores are averaged across both *male* and *female* identity classes.

Model	Base Model	Face Sim $\uparrow$	Robust Face Sim $\uparrow$	Relative Difference (%)
InstantID [29]	SD-XL [21]	80.17	71.33	-11.0%
	SD-XL Lightning [18]	82.91	74.77	-9.8%
PhotoMaker [17]	SD-XL	67.28	67.16	-0.2%
	SD-XL Lightning	66.67	63.02	-5.5%
PuLID [9]	FLUX.1-dev [15]	84.76	75.72	-10.7%
Rank-1 LoRA [10] + augmented inputs	FLUX.1-dev	64.32	61.41	-4.2%
	FLUX.1-dev	76.77	76.15	-0.8%
Meta-LoRA	FLUX.1-dev	79.45	77.16	-2.9%

## G Extra Metric Results

Table 5 presents a comparison of Meta-LoRA against state-of-the-art models from the literature, evaluated using the CLIP-T and R-FaceSim metrics. Meta-LoRA achieves the highest performance in facial similarity (R-FaceSim), establishing a new state-of-the-art in this aspect. For prompt adherence (CLIP-T), it ranks second, following PhotoMaker [17]. Notably, Meta-LoRA offers a more balanced trade-off between identity preservation and prompt alignment, whereas PhotoMaker tends to prioritize prompt fidelity at the expense of facial similarity.

Table 5: Quantitative comparison of our model with the state-of-the-art publicly available studies in the literature. The scores are taken for five seeds for both '*male*' and '*female*' subsets, and averaged to reach the final output. While CLIP-T is calculated from the Meta-PHD-FFHQ subset, R-FaceSim is computed using the Meta-PHD-Unsplash images. The 1st highest score is highlighted with **blue**, the 2nd with **red**, and the 3rd with **green**.

Model	Base Model	Train Dataset	CLIP-T (%) $\uparrow$	R-FaceSim (%) $\uparrow$
InstantID [29]	SD-XL [21]	60M	29.37	72.09
	SD-XL Lightning [18]		30.52	75.26
PhotoMaker [17]	SD-XL	112K	31.51	67.57
	SD-XL Lightning		31.92	63.51
PuLID [9]	FLUX.1-dev [15]	1.5M	30.95	75.72
Rank-1 LoRA + augmented inputs	FLUX.1-dev	0	31.63	61.41
	FLUX.1-dev		31.47	76.15
Meta-LoRA (ours)	FLUX.1-dev	8K (male), 21K (female)	31.66	77.16

## H Analysis on the *Male* Class Performance

The left panel of Figure 5 illustrates the distribution of R-FaceSim and CLIP-T scores for the '*male*' class across various hyperparameter configurations. Meta-LoRA consistently outperforms all baseline and previous state-of-the-art models, maintaining higher median and upper-bound scores. Compared to the female class, boundaries between different architectures (i.e., the performance gap) is easier to observe. Interestingly, even the baseline LoRA model demonstrates improved facial similarity compared to PuLID, suggesting that simpler adaptation methods can be competitive under certain conditions.

In Figure 5 (right), the plots show how CLIP-T and R-FaceSim scores vary with training iteration count. While the trends are similar to those observed for the *female* class (refer to the *Quantitative Results* section in the main paper), Meta-LoRA achieves a greater margin in R-FaceSim over prior state-of-the-art models when evaluated on the male subset.

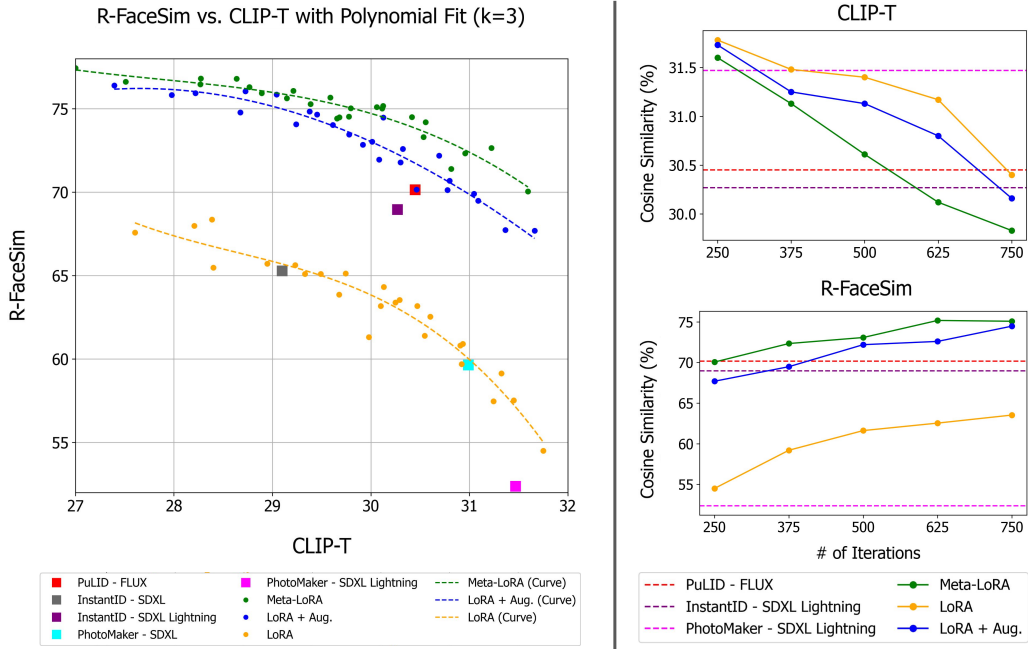


Figure 5: Illustration of the metric score trends for Meta-LoRA and the standard LoRA [10] models on the Meta-PHD dataset, focusing on the ‘male’ class. **Left:** A plot of R-FaceSim versus CLIP-T scores for all LoRA and Meta-LoRA models trained with ranks  $\in 1, 2, 4, 8, 16$  and across 250, 375, 500, 625, and 750 training iterations. The polynomial fit curves per each model are also shared for better comparison. **Right:** R-FaceSim and CLIP-T scores plotted against iteration count for rank-1 LoRA and Meta-LoRA models. These results are compared with state-of-the-art models from the literature, including PuLID [9], InstantID [29], and PhotoMaker [17]. To ensure a fair comparison, we use the FLUX.1-dev version of PuLID [15], which is consistent with the Meta-LoRA training setup. InstantID and PhotoMaker are based on SD-XL [21] and SD-XL Lightning [18], as public implementations of these models are not currently available for FLUX.1-dev.

## I Performance Curves on Different Ranks

Figure 6 analyzes the evolution of CLIP-T and R-FaceSim scores across different fine-tuning iterations (i.e., 250, 375, 500, 625, 750) and selected rank values (i.e., 1, 4, and 16). For both gender classes, increasing the rank generally leads to improved facial similarity (higher R-FaceSim) but at the cost of reduced prompt adherence (lower CLIP-T), indicating a tendency toward overfitting at earlier stages of training.

While CLIP-T scores show a noticeable gap between different ranks across all iteration counts, the variation in R-FaceSim narrows as the number of iterations increases for both Meta-LoRA and LoRA+aug. These trends suggest that lower ranks are better suited for achieving a balanced trade-off between identity preservation and prompt following, particularly in the context of final model evaluations.

## J Qualitative Results

Figures 7 and 8 demonstrate extended comparison for a diverse set of inputs and reference images.

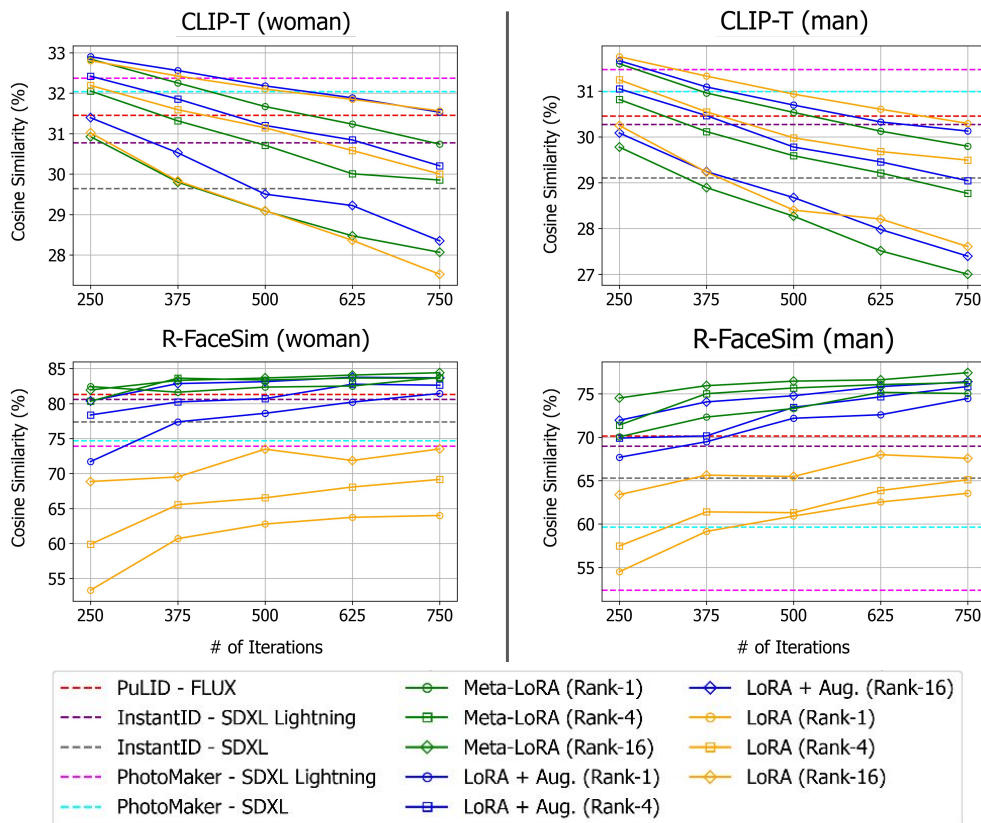


Figure 6: Visualization of CLIP-T and R-FaceSim performance for Meta-LoRA and baseline models across different fine-tuning iteration counts. The plots include results for both gender classes and three rank settings (i.e., 1, 4, and 16).

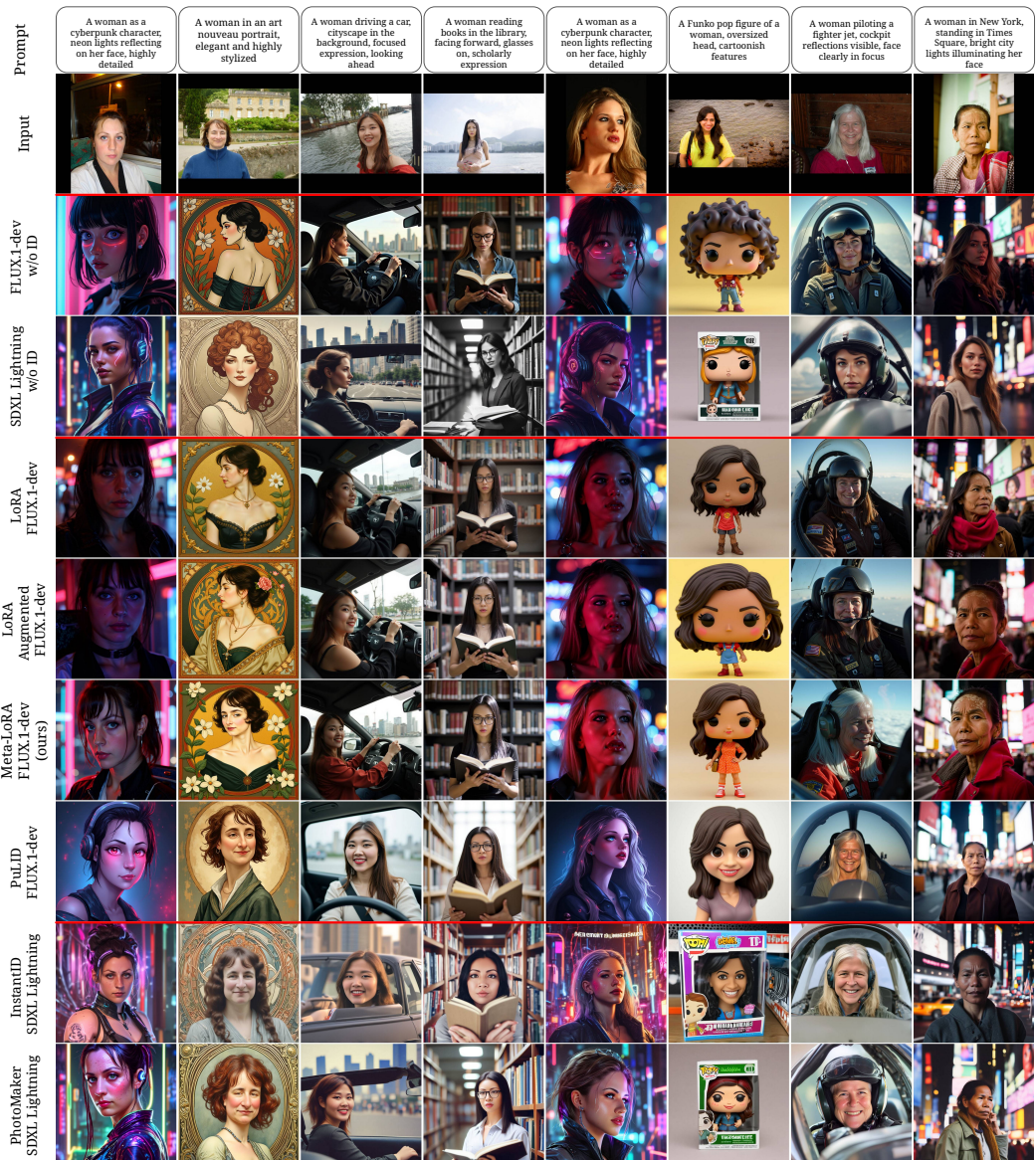


Figure 7: Qualitative comparisons for an extended list of baselines for woman identities.



Figure 8: Qualitative comparisons for an extended list of baselines for man identities.